SANDIA REPORT

SAND90—0153 • UC—405
Unlimited Release
Printed March 1990

A Vectorized Elastic/Plastic Power Law Hardening Material Model Including Lüders Strain

Charles M. Stone, Gerald W. Wellman, Raymond D. Krieg

Prepared by
Sandia National Laboratories
Albuquerque, New Mexico 87185 and Livermore, California 94550
for the United States Department of Energy
under Contract DE-AC04-76DP00789

Issued by Sandia National Laboratories, operated for the United States Department of Energy by Sandia Corporation.

Available to DOE and DOE contractors from
Office of Scientific and Technical Information
PO Box 62
Oak Ridge, TN 37831

Prices available from (615) 576-8401, FTS 626-8401

Available to the public from
National Technical Information Service
US Department of Commerce
5285 Port Royal Rd
Springfield, VA 22161

NTIS price codes
Printed copy: A03
Microfiche copy: A01

SAND--90-0153

DE90 010172

SAND90-01
Unlimited Release
Printed March 1990

Distribution
Category UC-405

A Vectorized Elastic/Plastic Power Law Hardening Material Model Including Lüders Strain

Charles M. Stone and Gerald W. Wellman
Applied Mechanics Division I
Sandia National Laboratories
Albuquerque, New Mexico 87185

Raymond D. Krieg
University of Tennessee
Knoxville, Tennessee 37996

Abstract

An elastic/plastic material model has been developed for use with the suite of Sandia Engineering Analysis Department finite element codes. This model describes post-yield strain hardening by a power law equation involving the equivalent plastic strain and includes a yield plateau or Lüders strain region. This combination of power law hardening and Lüders strain accurately represents the mechanical behavior of a large number of commonly used engineering materials. The material model is vectorized to take advantage of current super-computer architecture. The model shows only a modest increase in CPU time over the linear hardening material model currently in the codes. Several example problems are presented to show the accuracy and flexibility of the elastic/plastic power law hardening model.

Contents

Tables

Figures

Introduction

The nonlinear finite element codes developed by the Sandia Engineering Analysis Department contain similar constitutive models within their respective material libraries. The internal architecture of the codes is very similar, by design, in order to allow material models developed for one code to be easily implemented into the other codes. The most commonly used model in the material libraries is the elastic/plastic combined isotropic/kinematic hardening model. This model, which is based on the standard Von Mises yield criterion, uses the radial return method for integration of the rate equations. The radial return method, which is simple in concept and implementation, has been studied by several authors [1,2] and found to be very accurate for integrating elastic/plastic rate equations. The plasticity model commonly used in the Sandia suite of codes requires as input the usual elastic constants E and ν , which are Young's modulus and Poisson's ratio, respectively, the yield stress, σ_{ys}, and the hardening modulus, E_t. A final scalar parameter, β, which is called the hardening parameter, determines the proportion of kinematic or isotropic hardening in the combined model.

This model considers the hardening modulus to be a constant which means that the post-yield effective stress, $\bar{\sigma}$ *vs* effective plastic strain, $\bar{\epsilon}^p$, relationship is linear. For a large class of important problems, a linear $\bar{\sigma}$ *vs* $\bar{\epsilon}^p$ relationship may be adequate for the post-yield behavior over the strain range of interest. This, however, places a severe restriction on the materials to be modeled or requires *a priori* information about the expected strain levels in the problem so that an appropriate hardening modulus may be selected to produce a good approximation to the correct stress state based on the expected strain values. In addition, the strain range of interest must be small (no large strain gradients) so that the linear $\bar{\sigma}$ *vs* $\bar{\epsilon}^p$ relationship is applicable. However, there are classes of problems in which the linear approximation for plastic hardening is inadequate. A constant hardening modulus cannot adequately describe the post-yield behavior in order to predict structural behavior in the detail required. Determination of limit load response is an example of a class of problems for which linear hardening is inappropriate.

In order to overcome these restrictions, a variable hardening plasticity model has been developed for the Sandia developed finite element codes **JAC**[3], **JAC3D**[4], **SANTOS**[5], **PRONTO 2D**[6], and **PRONTO 3D**[7]. The use of piecewise linear segments to represent the hardening curve was an initial consideration based on the capability to match any material hardening behavior, but the resulting material model subroutine was not amenable to vectorization. Vectorization requirements limit the form of the model to a functional relationship between effective stress and effective plastic strain. The form of the current implementation considers the post-yield stress to be described by a power law involving the equivalent plastic strain with the option to include a Lüders strain

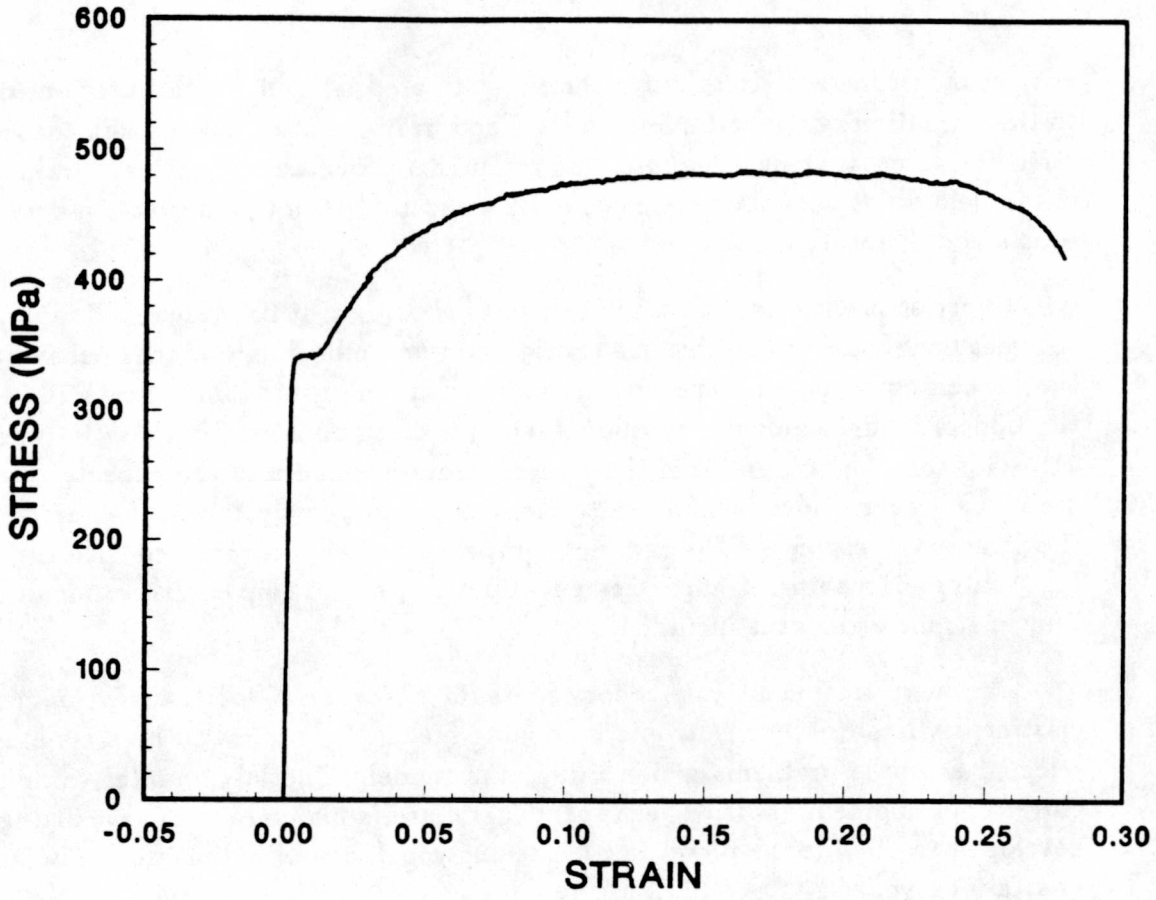

Figure 1. Stress *vs* Strain Curve for a Typical Ferritic Steel Exhibiting Lüders Strain

segment. The form of the hardening model was selected for its simplicity and ability to match the post-yield behavior of many engineering materials. The model has the form during a plastic loading process

$$\bar{\sigma} - \sigma_{ys} = A \left\langle \bar{\epsilon}^p - \epsilon^L \right\rangle^n \tag{1}$$

where A and n are material constants, $\bar{\epsilon}^p$ is the equivalent plastic strain, $\bar{\sigma}$ is the effective stress, σ_{ys} is the initial yield stress, and ϵ^L is the Lüders strain or yield plateau strain. The use of brackets, <>, in Equation (1) denotes the use of a Heaviside function. The function is zero until the arithmetic expression within the brackets becomes positive. The material constants can be determined from measured stress *vs* strain data through simple curve fitting techniques (see the Appendix). By suitably choosing the material constants A and n, the form of the model can represent either elastic/perfectly plastic or linear hardening material behavior in addition to the power law hardening response. The proposed material model is strictly valid for isotropic hardening behavior where the radius of the yield surface grows equally in all directions due to plastic straining.

Many engineering materials exhibit the phenomenon of Lüders straining. A typical stress *vs* strain curve for such a material is shown in Figure 1. In reality, Lüders strain does

not occur at constant stress but rather in a serrated fashion. Each serration corresponds to the formation of a new Lüders band. The serrations are small enough that a constant stress representation is adequate. In common ferrous alloys, Lüders strain as well as other yield point phenomena are generally associated with the interaction between solute atoms and dislocations.

Experience with implicit finite element codes that utilize Newton-Raphson solution schemes has shown difficulties in convergence when modeling material behavior in which the hardening modulus increases. Since the hardening modulus always increases after the Lüders strain segment, the Lüders strain is often omitted from elastic/plastic analyses. This may be acceptable if the Lüders strain is small and the expected strain levels are much greater, however, for many problems the Lüders strain will significantly affect the structural response. The indirect solution schemes incorporated into the Engineering Analysis Department finite element codes exhibit no convergence difficulties when a Lüders strain segment is included.

The next section of this report presents an overview of the development of the elastic/plastic power law isotropic hardening model. It is followed by a chapter showing selected example problems which utilize the model. The last chapter summarizes the current development effort. The Appendix is a user's manual for a curve fitting program developed to provide the power law hardening constants, A and n, from a uniaxial stress *vs* strain curve.

Model Development

The purpose of this section is to describe the development of the elastic/plastic power law isotropic hardening material model and to document the underlying assumptions and the numerical implementation. The unique aspect of this model is that it accommodates the presence of Lüders strain in the measured stress *vs* strain curve. The current value of the yield stress, $\bar{\sigma}_y$, can be determined from

$$\bar{\sigma}_y = \sigma_{y_0} + A \left\langle \bar{\epsilon}^p - \epsilon^L \right\rangle^n \tag{2}$$

where σ_{y_0} is the initial yield stress, $\bar{\epsilon}^p$ is the equivalent plastic strain, ϵ^L is the specified Lüders strain, and A and n are material parameters determined by fitting the model to elastic/plastic data. For equivalent plastic strain values less than ϵ^L, the current value of the yield stress is equal to the initial yield stress.

In the following development, effective or equivalent scalar quantities are capped with a bar and tensor quantities are denoted using conventional summation notation. The constitutive routine is entered with the stress state at the beginning of the step, σ_{ij}^{old}, the total strain rate, $\dot{\epsilon}_{ij}$, and the time step size, Δt. The value of the yield stress, $\bar{\sigma}_y$, and the equivalent plastic strain, $\bar{\epsilon}_0^p$, computed at the last step are available as state variables. An elastic trial stress for the step is computed as

$$\sigma_{ij}^{tr} = \sigma_{ij}^{old} + (\lambda \, \dot{\epsilon}_{kk} \, \delta_{ij} + 2 \, \mu \, \dot{\epsilon}_{ij}) \, \Delta t \, . \tag{3}$$

where λ and μ are the Lamé parameters, and δ_{ij} is the Kronecker delta. In this model a von Mises yield criterion is used where the equivalent or effective trial stress, $\bar{\sigma}^{tr}$, is defined by

$$\bar{\sigma}^{tr} = \sqrt{\frac{3}{2} \, S_{pq}^{tr} \, S_{pq}^{tr}} \, . \tag{4}$$

The term S_{pq}^{tr} refers to the deviatoric components of the trial stress. The effective trial stress is compared to the current value of the yield stress and if $\bar{\sigma}^{tr} \leq \bar{\sigma}_y$ then the step is elastic and the trial stress is the final stress. Otherwise, yielding occurs during the step and the radial return algorithm is used to compute the final deviatoric stress state, S_{ij}^f, as

$$S_{ij}^f = S_{ij}^{tr} \, \frac{\bar{\sigma}^f}{\bar{\sigma}^{tr}} \tag{5}$$

where $\bar{\sigma}^f$ still remains to be determined. The plastic strain increments associated with the process can be computed as

$$\Delta \epsilon_{ij}^p = \frac{S_{ij}^{tr} - S_{ij}^f}{2\mu} \tag{6}$$

which can be rewritten as

$$\Delta\epsilon_{ij}^{p} = \frac{1}{2\mu}\left(1 - \frac{\bar{\sigma}^{f}}{\bar{\sigma}^{tr}}\right) S_{ij}^{tr}\,. \tag{7}$$

This tensor equation may be converted to a scalar equation by taking an inner product with itself. The scalar equation may then be combined with the definitions of effective stress, equation (4), and effective plastic strain

$$\Delta\bar{\epsilon}^{p} = \sqrt{\frac{2}{3}\,\Delta\epsilon_{ij}^{p}\,\Delta\epsilon_{ij}^{p}} \tag{8}$$

to produce an expression for the effective plastic strain increment

$$\Delta\bar{\epsilon}^{p} = \frac{\bar{\sigma}^{tr} - \bar{\sigma}^{f}}{3\mu} \tag{9}$$

which contains the still undetermined $\bar{\sigma}^{f}$. The increment of effective plastic strain can now be added to $\bar{\epsilon}_{0}^{p}$ to get $\bar{\epsilon}^{p}$ which when substituted into equation (2) produces the final form for $\bar{\sigma}^{f}$

$$\bar{\sigma}^{f} = \sigma_{y_0} + A\left\langle \bar{\epsilon}_{0}^{p} + \frac{\bar{\sigma}^{tr} - \bar{\sigma}^{f}}{3\mu} - \epsilon^{L} \right\rangle^{n}. \tag{10}$$

This nonlinear equation is solved for $\bar{\sigma}^{f}$ using a fixed number of Newton-Raphson iterations to preserve the vectorization. Comparison of input and computed stress *vs* strain curves for several sample problems has shown that three iterations are sufficient to produce an accurate value of $\bar{\sigma}^{f}$. This value may then be used to compute the increment of effective plastic strain occurring over the step, Equation (9), as well as the final deviatoric stress state, S_{ij}^{f} from Equation (5).

The model is implemented to take advantage of the vector architecture of the CRAY computer. The constitutive model is called with the total strain rates for the step and the stress from the previous step as input. Processing is done on a maximum block size of 64 elements at a time incorporating a single FORTRAN loop. There are two internal variables stored at each step for every element. These are the current radius of the yield surface and the current value of the equivalent plastic strain. Timing studies have shown that the execution time (CPU time/element/iteration) for the power law hardening model increased 13 percent compared with execution times for the linear hardening model.

Example Problems

Three example problems were selected to demonstrate the accuracy and flexibility of the elastic/plastic power law hardening material model described above. The first example shows a comparison between the numerical results using this material model and a closed form analytical solution of the problem of a pressurized hollow sphere. The second example demonstrates the ability of this material model to accurately represent the load-displacement behavior of a tensile specimen experiencing large geometry and large strain effects. Finally, the third example demonstrates the broad range of material response available with the elastic/plastic power law hardening model.

Hollow Sphere with Internal Pressure

An analytical solution has been found for an internally pressurized, hollow sphere characterized by an elastic/plastic power law isotropic hardening material [8]. The hollow sphere has an inner to outer diameter ratio of 2, with the dimensions shown in Figure 2. The non-dimensional material constants used in the analysis are shown in Table 1. An axisymmetric analysis was performed using the finite element analysis code, **SANTOS**. Analytic values of plastic strain as a function of sphere radius are compared to the numerical solution from **SANTOS** in Figure 3 for various internal pressures. The numerical solution is represented in the figure by the solid lines. The solution is characterized by a large gradient in plastic strain which occurs at the inner radius. The agreement between the analytic and numerical models is extremely good at all locations through the radius for the range of applied pressure.

Table 1. Material Properties Used for Hollow Sphere Analysis

Young's Modulus	Poisson's Ratio	Yield Stress	Hardening Constant, A	Hardening Exponent, n	Lüders Strain
31.0×10^6	0.3	$30. \times 10^3$	3.0×10^5	0.5	0.0

Standard Tension Test

The ability to reproduce observed mechanical behavior provided the primary impetus to the development of this new material model. The standard tension test is perhaps the most familiar mechanical behavior in engineering. The intent of this example problem

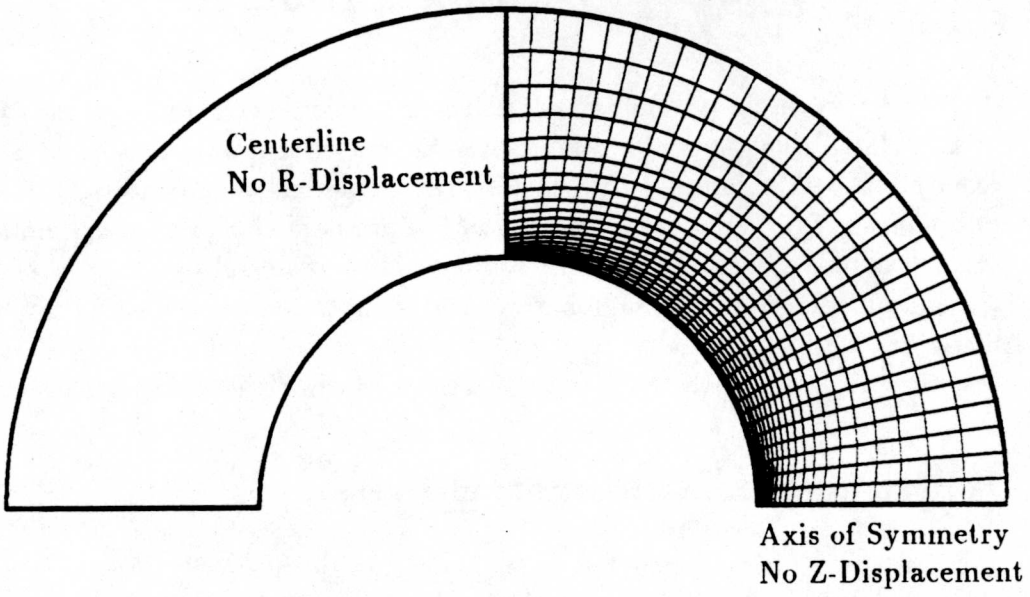

Figure 2. Description of the Internally Pressurized Hollow Sphere Example Problem

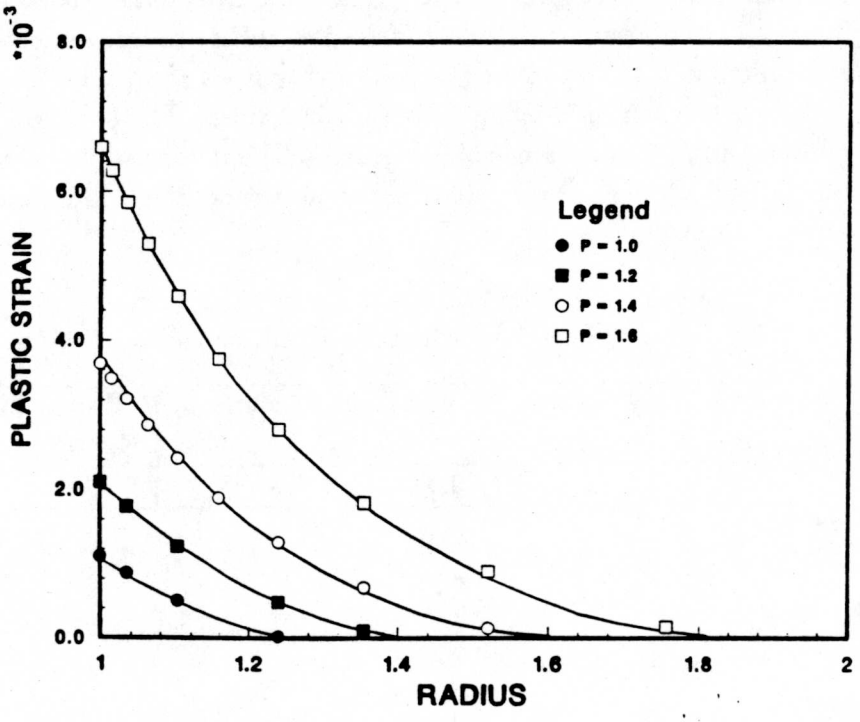

Figure 3. Variation of Plastic Strain With Radius for Several Values of Internal Pressure; Pressure Has Been Normalized With Respect to the Material Yield Stress

Table 2. GGG-40 Material Properties Used for Tension Test Analysis

Young's Modulus (GPa)	Poisson's Ratio	Yield Stress (MPa)	Hardening Constant, A (MPa)	Hardening Exponent, n	Lüders Strain
182.7	0.3	132.4	508.2	0.319	0.0

was to take the material's true stress *vs* true strain behavior, and reproduce the load *vs* displacement response of the tensile test, including peak load and unloading behavior. During the tension test, the specimen experiences large geometry changes in addition to the nonlinear material response. When the specimen softening due to the geometric reduction in cross-section area matches the specimen stiffening from the material strain hardening, peak load is reached. After this point a local tensile instability or necking will result. Thus, the determination of peak load is controlled by the interaction between the specimen geometry and the material nonlinear response. The true stress *vs* true strain curve input provided to the model does not include any information regarding peak load or unloading, see Figure 5, curve (c).

The tensile test geometry considered is shown in Figure 4. An axisymmetric analysis of the 6.35 mm diameter tensile test specimen was performed using the finite element analysis code, **SANTOS**. Making use of symmetry, only the top half of the specimen was modeled. In order to force the necking to initiate at the center of the gage length, the diameter of the model was arbitrarily reduced to 6.29 mm to provide an initial geometric imperfection at the plane of symmetry.

A ductile cast iron material (nominally GGG-40) was selected for use in this example. The engineering stress *vs* engineering strain tensile test results for a gage length of 25.4 mm are shown in Figure 5. The true stress *vs* true strain curve, up to peak load, was estimated assuming a uniform decrease in radius over the length of the specimen and assuming constant volume plasticity [9] according to the following:

$$\epsilon_{true} = \ln(\epsilon_{eng} + 1) \tag{11}$$

$$\sigma_{true} = \sigma_{eng}(\epsilon_{eng} + 1)\,. \tag{12}$$

The power law constants, A and n, were extracted by performing a least squares fit to the true stress *vs* true strain curve as described in the Appendix. Thus, the power law hardening true stress *vs* true strain behavior has been extrapolated beyond peak load. The material constants used in the analysis are shown in Table 2. The true stress *vs* true strain curves estimated from equations 10 and 11 and from the power law description are also shown in Figure 5.

The tensile test load *vs* displacement curve from the finite element analysis is compared with that from the experiment in Figure 6. The agreement between experiment

Table 3. Material Properties Used for Analysis of Plate with a Central Hole

	Young's Modulus (GPa)	Poisson's Ratio	Yield Stress (MPa)	Hardening Constant, A (GPa)	Hardening Exponent, n	Lüders Strain
Case A	207.	0.3	207.	0.00	1.0	1.0
Case B	207.	0.3	207.	2.07	1.0	0.0
Case C	207.	0.3	207.	2.07	0.5	0.0
Case D	207.	0.3	207.	2.07	0.5	0.05

and analysis is very good with the predicted peak load within 0.5 percent of the measured value. The predicted peak load does occur at a larger displacement than observed in the experiment. The accuracy of the peak load calculation could not be obtained using a linear hardening model. The prediction of peak load and the onset of the instability is controlled by the local material tangent modulus and the rate of change of the cross-section area, which is a function of plastic strain. The variable hardening provided by the power law representation is the key to this comparison. The analytical deformed shape showing the necking behavior is shown in Figure 7 for a specimen displacement of 10.66 mm.

Plate with Central Hole Loaded in Tension

The intent of this example problem is to show the variations in behavior possible with this material model. Four material descriptions (stress *vs* strain curves) were considered: elastic/perfectly plastic, elastic/plastic linear hardening, elastic/plastic power law hardening, and elastic/plastic power law hardening with Lüders strain. All four material characterizations can be represented by the material model described in this report by suitably choosing the power law constants. The tensile plate with a central hole geometry was selected because it has a simply described global behavior (remote load *vs* displacement) which is controlled by a more complex local behavior (non-linear stress and strain gradients along the plate centerline from the edge of the hole to the plate free surface).

Two-dimensional, plane-strain analyses including large geometry change assumptions were performed on the plate. The plate had the following dimensions: half length of 2 m, half width of 1 m, and hole radius of 0.25 m. Because of symmetry conditions, only one fourth of the plate needed to be modeled, as shown in Figure 8. Kinematic boundary conditions were used to enforce the symmetry conditions. The four stress *vs* strain curves assumed for the analyses are shown in Figure 9. The value of the hardening constant for the elastic/plastic linear hardening model was determined by requiring the effective stress at an equivalent plastic strain of 1.0 to match the effective stress

determined from the elastic/plastic power law hardening model.

The plate was loaded by imposing uniform vertical displacements along the top edge. Displacement control loading enhances the stability of the solution algorithm, particularly under the conditions of decreasing load. The sum of the nodal reactions along the horizontal symmetry plane provides the value of total load applied to the plate. Figure 10 shows the four load *vs* displacement curves corresponding to the four stress *vs* strain curves. The plotted value of displacement corresponds to the imposed vertical displacement along the top edge. Curve (a) shows decreasing load with increasing vertical displacement which reflects the response for an elastic/perfectly plastic material. The cross-sectional area of the plate begins to decrease with the onset of plastic straining and with no compensation from strain hardening, the total load decreases. The response at small displacements shown in curves (b), (c), and (d) reflects the onset of yielding at the edge of the hole and subsequent spread of the yield zone across the plate ligament. After yielding of the entire ligament, the response of the plate is dominated by the specified stress *vs* strain behavior.

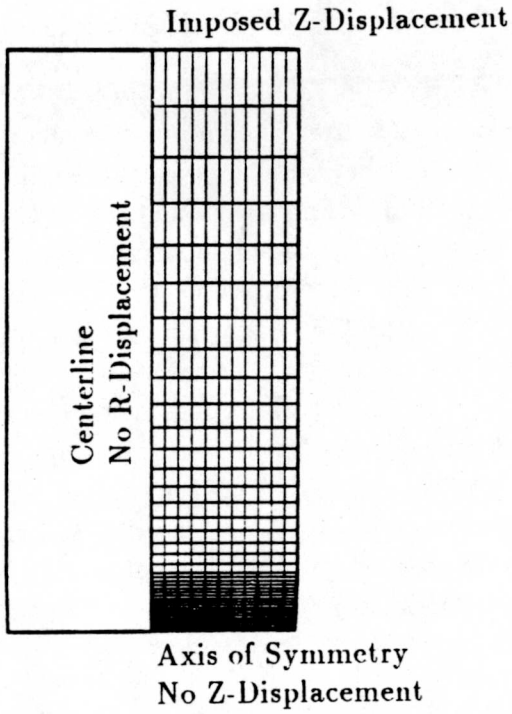

Figure 4. Description of the Standard Tension Test Example Problem

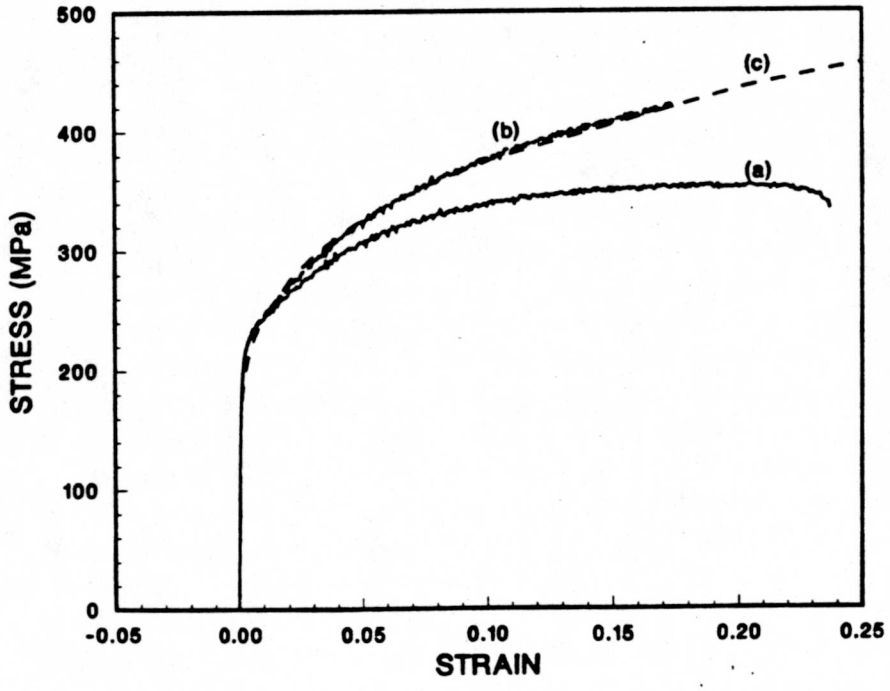

Figure 5. Stress *vs* Strain Curves Representing GGG-40 Material Behavior: a) Engineering Stress *vs* Engineering Strain (Experimental), b) True Stress *vs* True Strain (Estimated from Equations 10 and 11), c) Power Law Hardening Fit to True Stress *vs* True Strain

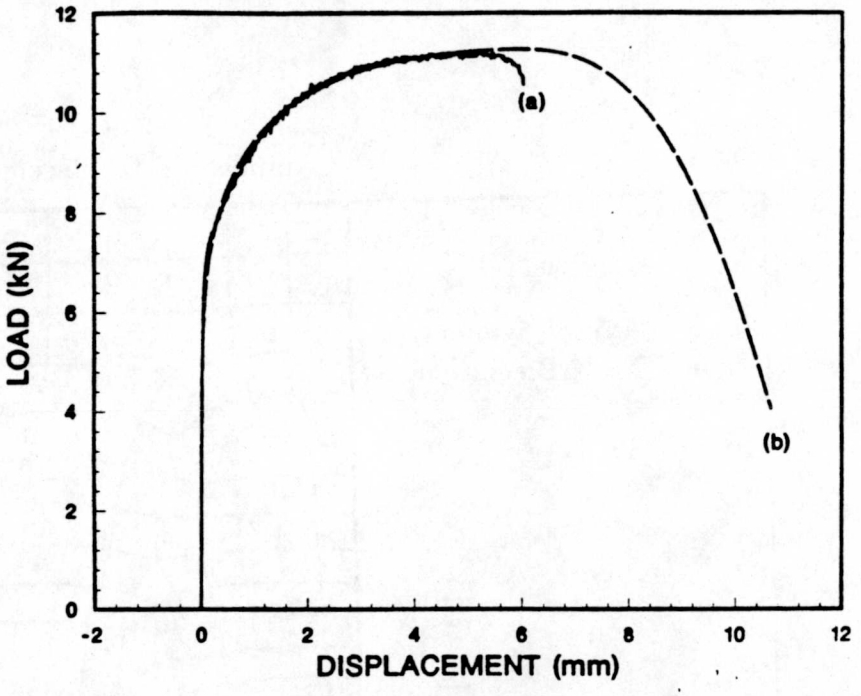

Figure 6. Comparison of the Load *vs* Displacement Results for the Tensile Test Example Problem: a) Experimental, b) Analytical

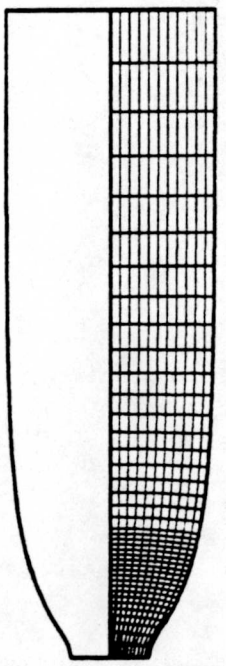

Figure 7. Deformed Shape of the Tensile Test Example Problem Showing the Necking Behavior

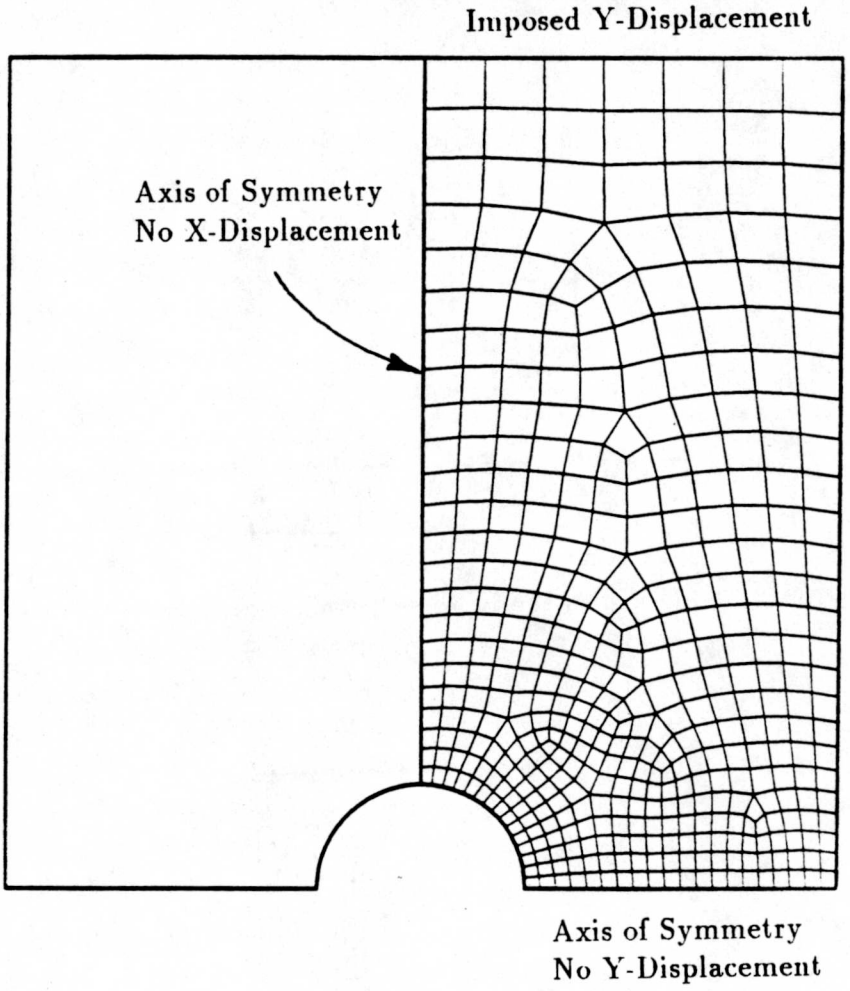

Figure 8. Description of the Plate with a Central Hole Example Problem

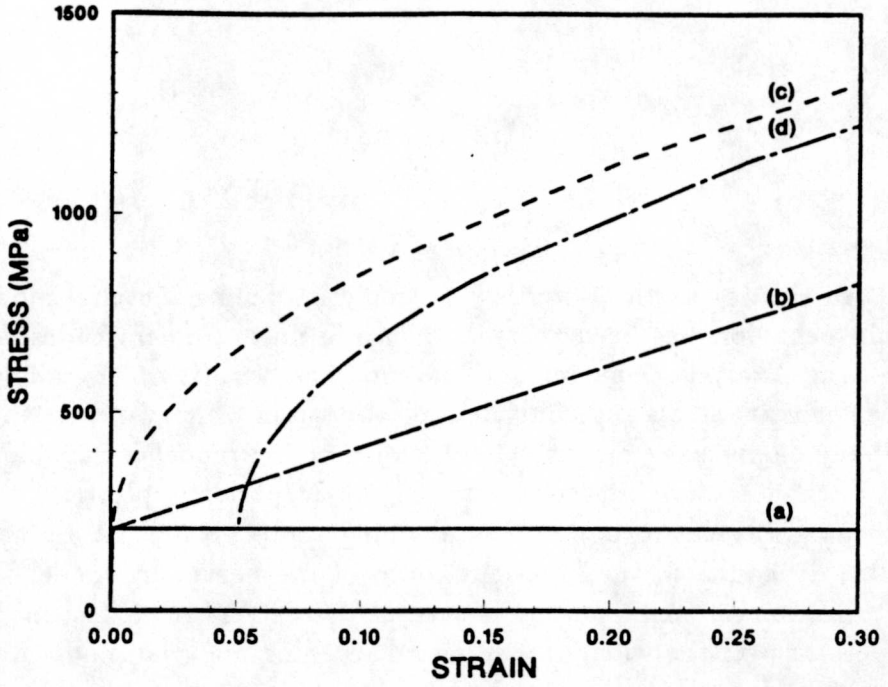

Figure 9. Stress *vs* Strain Curves Used in the Analysis of the Plate with a Central Hole: a) Elastic/Perfectly Plastic, b) Elastic/Plastic Linear Hardening, c) Elastic/Plastic Power Law Hardening, d) Elastic/Plastic Power Law Hardening with Lüders Strain

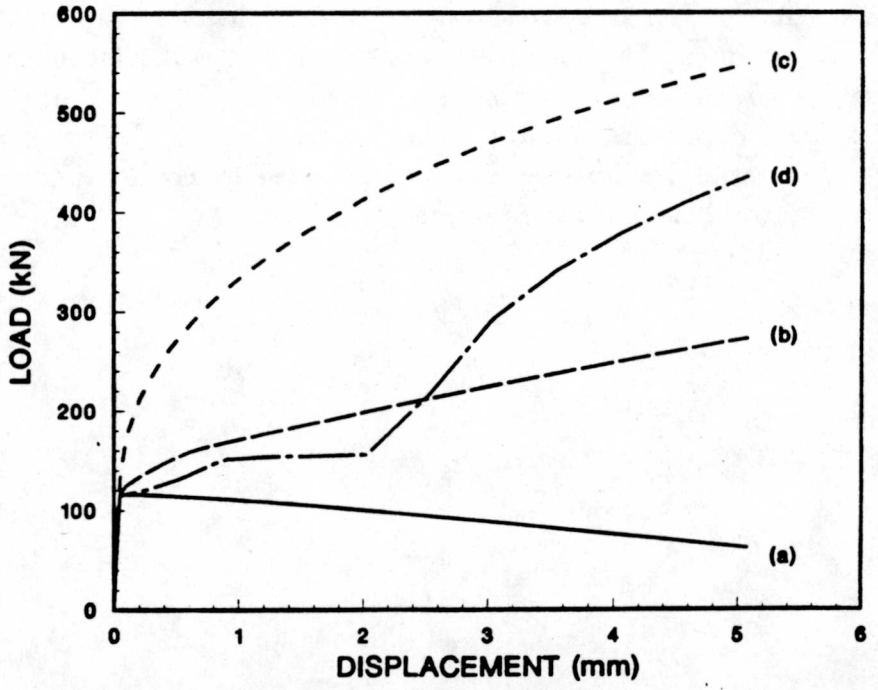

Figure 10. Comparison of Load *vs* Displacement Curves for the Plate with a Central Hole: a) Elastic/Perfectly Plastic, b) Elastic/Plastic Linear Hardening, c) Elastic/Plastic Power Law Hardening, d) Elastic/Plastic Power Law Hardening with Lüders Strain

Summary

An elastic/plastic power law isotropic hardening material model, including Lüders strain behavior, has been written for use in finite element codes developed by the Engineering Analysis Department. The model is based on a functional representation between effective stress and equivalent plastic strain which captures the hardening response of many engineering materials. The form of the model is capable of representing several distinct material descriptions: (1) elastic/perfectly plastic, (2) elastic/linear strain hardening, (3) elastic/power law hardening and (4) elastic/strain hardening with Lüders strain. In addition, the functional form of the hardening model lends itself readily to vectorization for supercomputers such as the CRAY. A modest increase in CPU time of 13 percent over the widely used linear hardening material model was observed.

The accuracy of the model was demonstrated by comparing numerical results with analytic results for an internally pressurized hollow sphere characterized by an elastic/plastic power law hardening material. Agreement between theory and the model was shown to be excellent. The advantage of the power law hardening material model over linear hardening was demonstrated by considering the response of a standard tension test specimen. The true stress *vs* true strain behavior of a ductile cast iron (GGG-40) was used as input. The measured tensile test load *vs* displacement curve compared very closely to the curve determined from the analysis. The computed peak load was within 0.5 percent of the measured value. The flexibility of the material model to represent several material descriptions was demonstrated by considering the response of a plate with a central hole loaded in tension.

References

1. R. D. Krieg and D. B. Krieg, "Accuracies of Numerical Solution Methods for the Elastic-Perfectly Plastic Model," *ASME Journal of Pressure Vessel Technology*, Vol. 99, 1977, pp 510-515.

2. H. L. Schreyer, R. F. Kulak and J. M. Kramer, "Accurate Numerical Solutions for Elastic-Plastic Models," *ASME Journal of Pressure Vessel Technology*, Vol. 101, 1979, pp 226-234.

3. J. H. Biffle, "JAC - A Two-Dimensional Finite Element Computer Program for the Non-Linear Quasistatic Response of Solids with the Conjugate Gradient Method," SAND81-0998, Sandia National Laboratories, Albuquerque, New Mexico, April 1984.

4. J. H. Biffle, "JAC3D - A Three-Dimensional Finite Element Computer Program for the Nonlinear Quasi-Static Response of Solids with the Conjugate Gradient Method," SAND87-1305, Sandia National Laboratories, Albuquerque, New Mexico, in preparation.

5. C. M. Stone, "SANTOS A Two-Dimensional Finite Element Program for the Quasistatic, Large Deformation, Inelastic Response of Solids," SAND90-0543, Sandia National Laboratories, Albuquerque, New Mexico, in preparation.

6. L. M. Taylor and D. P. Flanagan, "PRONTO 2D A Two-Dimensional Transient Solid Dynamics Program," SAND86-0594, Sandia National Laboratories, Albuquerque, New Mexico, March 1987.

7. L. M. Taylor and D. P. Flanagan, "PRONTO 3D A Three-Dimensional Transient Solid Dynamics Program," SAND87-1912, Sandia National Laboratories, Albuquerque, New Mexico, March 1989.

8. A. Mendelsohn, *Plasticity: Theory and Application*, The Macmillan Co., New York, 1968, pp 150-153.

9. G. E. Dieter, *Mechanical Metallurgy*, 2nd ed., McGraw-Hill Book Co., New York, 1976, p 337.

10. D. J. Segalman and C. R. Dohrmann, private communication, Sandia National Laboratories, Albuquerque, New Mexico, November 1989.

11. W. H. Press, B. P. Flannery, S. A. Teukolsky, and W. T. Vetterling, *Numerical Recipes, The Art of Scientific Computing*, Cambridge University Press, New York, 1986, pp 504-509.

12. C. R. Adams, "GRAFAID Code User Manual - Version 2.0," SAND84-1725, Sandia National Laboratories, Albuquerque, New Mexico, September 1985.

Appendix
User's Manual for PLHFIT: a Program to Calculate the Power Law Constants A and n

PLHFIT is a computer program to aid analysts in determining the power law coefficients A and n which describe the post yield mechanical behavior of their material. The program calculates A and n from a regression analysis of a user supplied set of stress/strain data pairs. The details of the regression algorithm are given the following section. Subsequent sections describe the execution procedure, the input format, and the format of the results.

Description of the Regression Algorithm

The user supplied stress/strain data pairs are to be fit to a power law equation of the form

$$\bar{\sigma} - \sigma_{y_s} = A \left\langle \bar{\epsilon}^p - \epsilon^L \right\rangle^n . \tag{A.1}$$

As implied by the Heaviside brackets, only the hardening portion of the stress *vs* strain curve is used to determine the power law coefficients A and n. Therefore, the strain data are manipulated to extract the plastic component of strain from the total strain. Then all data pairs which have a stress less than the yield stress or which have a plastic strain less than the Lüders strain are eliminated. Thus, only positive values of the quantities $(\bar{\sigma} - \sigma_{y_s})$ and $(\bar{\epsilon}^p - \epsilon^L)$ remain. The power law (equation A.1) can be rewritten as a linear equation in terms of the logarithms of the stress and plastic strain difference quantities.

$$\ln\left(\bar{\sigma} - \sigma_{y_s}\right) = \ln A + n \times \ln\left(\bar{\epsilon}^p - \epsilon^L\right) \tag{A.2}$$

Rather than simply performing a least squares linear regression on equation A.2, two weighting parameters are introduced. The first weighting parameter reduces the effect of variable data spacing on the regression results. The data are weighted by the difference in the strain values. This weighting scheme tends to minimize the difference in area between the experimental and regression curves rather than the differences at individual data points. This weighting also introduces the requirement that the data pairs be monotonic. Since stress/strain data are typically monotonic, this requirement is not particularly restrictive. The second weighting parameter corrects for the inaccuracy that results from performing the regression on the logarithms of the data rather than on the original data. The least squares procedure minimizes the square of the difference between the actual data, y, and the evaluation of the function, $\hat{y}$, see expression A.3.

$$\min \sum (y - \hat{y})^2 \tag{A.3}$$

By using logarithms of the data, the procedure actually minimizes the differences in logarithms,

$$\min \sum (\ln y - \ln \hat{y})^2 \ . \tag{A.4}$$

Minimizing the differences in logarithms rather than the actual values, implicitly results in giving greater weight to smaller data values than is given to larger data values. Using $1/y^2$ as a weighting parameter approximately corrects this implicit weighting as shown below [10]. Taking the first two terms of the Taylor series expansion for expression A.4,

$$\sum (\ln y - \ln \hat{y})^2 \approx \sum \left(\frac{y - \hat{y}}{y} \right)^2 \tag{A.5}$$

The difference between expression A.3 and the right hand side of equation A.5 is simply $1/y^2$, the weighting parameter. The power law coefficients are then calculated using a standard least squares weighted linear regression technique [11].

Execution of PLHFIT

The **PLHFIT** executable and source files are located on the 1500 VAX cluster. The **PLHFIT** program is run by typing:

PLHFIT *input_file*

where *input_file* is the name of the file containing the stress-strain input data. The file extension for this file must be .INP. **PLHFIT** does not allow the input data to be entered interactively.

Input Format for PLHFIT

The data input format used by **PLHFIT** is a free field form using keywords. The keywords are intended to define a user friendly program language input. The free field input allows the user to delimit entries by either a blank, a comma, or an equals sign. A dollar sign indicates that whatever follows on the line of input is a comment and is ignored. The keyword parsing system used in **PLHFIT** examines keywords until an unambiguous entity results. All subsequent character data are ignored. Once an unambiguous keyword entity has been identified, the first numerical constant is accepted. After a keyword and a numerical constant have been accepted, the remainder of the command line is ignored. The keywords may be entered in any order. The entry of the data pairs which define the stress/strain curve is a slight exception to the description above. The keyword which defines the beginning of the stress/strain data pair entry has no numerical value associated with it. When identified, this keyword transfers the free field reader to a location where it will accept two numerical constants (strain value, stress value) per line without any keyword until the keyword which defines the end of

Table A.1. List of Keywords Recognized by **PLHFIT**

YOUngs modulus or E	The elastic modulus of the material
YIEld STRess	The yield strength of the material
LUDers strain or YIEld PLAteau	The plastic strain offset from the yield point to the start of the strain hardening region
DATa	Sets the parser to commence reading data pairs in STRAIN; STRESS order
END DATa	Sets the parser to return to reading KEYWORD; NUMERICAL CONSTANT input
END or EXIt	Defines the end of the input data

the stress/strain data is identified. At this point, the command line parsing reverts to its initial description (keyword followed by numerical value). The stress/strain data pairs must define a monotonic curve. This requirement is due to the weighting values assigned based on the spacing of the strain values explained in the previous section.

A list of keywords recognized by **PLHFIT** is provided in Table A.1. All keywords are required and no default values are assumed. Typically, keywords are parsed for the first three characters. The convention used in Table A.1 is, capital letters in the keyword are required; lower case characters are optional. If an unacceptable or unrecognizable keyword is read, **PLHFIT** prints an error message and aborts. The program will check that all required information has been entered. If not, the missing keyword will be printed and the program will abort. In all cases, a complete echo of the input data is printed. A sample input deck is presented in Figure A.1.

Output from PLHFIT

Two files are created during the execution of **PLHFIT**. One file is a text file containing an echo of the input data followed by the calculated power law coefficients. The

```
E = 23.1E06
YIELD STRESS = 19200
LUDERS STRAIN = 0.
DATA
7.996935-4,18604.1699
9.745377-4,21513.2402
  .
  .
  .
0.17206070,60915.0508
0.17269200,61135.1094
END DATA
EXIT
```

Figure A.1. Sample input deck for PLHFIT

other file contains the stress/strain data pairs which define two curves in **GRAFAID** [12] neutral file format. The first curve is an echo of the stress/strain input data. The second curve contains stress/strain data pairs calculated using the power law coefficients. It is strongly recommended that these two curves be examined graphically so that the user may determine the suitability of the power law curve for his purpose. In certain cases, it has been found to be beneficial to eliminate some of the small strain data when a good fit to the large strain data is required.

The text file name is the same as the input file name with a .OUT extension. The **GRAFAID** neutral file has the extension .NEU with the same file name as that used for the input file. For example, if **PLHFIT** is successfully run with an input file of CURVE.INP, a text file named CURVE.OUT and a **GRAFAID** neutral file named CURVE.NEU will be created.

Distribution:

Raymond D. Krieg (10)
Engineering Sciences and Mechanics
301 Perkins Hall
The University of Tennessee
Knoxville, TN 37996-2030

1510 J. W. Nunziato
1520 L. W. Davison
1521 H. S. Morgan
1521 J. G. Arguello
1521 S. W. Attaway
1521 V. L. Bergmann
1521 S. N. Burchett
1521 M. K. Neilsen
1521 G. D. Sjaardema
1521 J. R. Weatherby
1522 R. C. Reuter
1523 J. H. Biffle
1523 R. S. Chambers
1523 E. P. Chen
1523 J. Jung
1524 D. R. Martinez
1524 C. R. Dohrmann
1530 J. R. Asay
1550 C. W. Peterson
1831 J. J. Stephens Jr.
1832 W. B. Jones
1832 R. J. Bourcier
1832 R. J. Salzbrenner
2513 D. E. Mitchell
2515 P. D. Wilcox
2543 K. G. McCaughey
3141 S. A. Landenberger (5)
3141-1 C. L. Ward (8) For: DOE/OSTI
3151 W. I. Klein (3)
6322 J. E. Stiegler (acting)
6322 K. B. Sorenson
6523 W. A. von Riesemann
6523 M. B. Parks
7230 J. F. Ney
8241 M. L. Chiesa
8243 M. L. Callabresi
8243 D. J. Bammann
8524 J. A. Wackerly
1521 C. M. Stone (10)
1521 G. W. Wellman (10)